

## Rare earth geochemistry of Arenig cherts from the Ballantrae Ophiolite and Leadhills Imbricate Zone, southern Scotland: implications for origin and significance to the Caledonian Orogeny

H. A. ARMSTRONG<sup>1</sup>, A. W. OWEN<sup>2</sup> & J. D. FLOYD<sup>3</sup>

<sup>1</sup>Department of Geological Sciences, University of Durham, South Road, Durham DH1 3LE, UK

<sup>2</sup>Department of Geology and Applied Geology, University of Glasgow, Lilybank Gardens, Glasgow G12 8QQ, UK

<sup>3</sup>British Geological Survey, Murchison House, West Mains Road, Edinburgh EH9 3LA, UK

**Abstract:** Rare earth element (REE) data from low to mid-Arenig cherts are used to test competing models for the early Ordovician evolution of the Laurentian margin in the northern British Isles. Cherts from the Ballantrae Ophiolite Complex have chondrite-normalized REE patterns typical of continental margin settings with LREE enrichment, a slight negative  $Eu_{anom}$  and shale and chondrite-normalized La/Yb values of 0.97–1.41 and 7.78–11.4 respectively. This pattern, together with a large positive chondrite-normalized  $Ce_{anom}$  (1.44–1.70), is virtually identical to that found in radiolarian chert of the Gascoyne Abyssal Plain, in the Timor Sea. Cherts from the Raven Gill Formation within the Leadhills Imbricate Zone, Northern Belt, Southern Uplands have typical continental margin REE patterns, chondrite-normalized  $Ce_{anom}$  (0.9–1.21) and  $Eu_{anom}$  (0.61–0.79) values indicating that they formed closer to the continental margin than those from Ballantrae. Shale and chondrite-normalized and La/Yb values of 0.95–1.27 and 4.92–13.88 respectively confirm this interpretation.

It is concluded that the Ballantrae ophiolite formed in a rifted–arc basin above a northwards dipping, intra-oceanic subduction zone. The modest depth of burial of the Raven Gill Formation precludes it being part of a marginal basin which was subsequently trapped as the Ballantrae Ophiolite was obducted in the late Arenig. The Arenig rocks of the Leadhills Imbricate Zone represent an allochthonous terrane accreted to the western extension of the Midland Valley in Ireland in pre-Caradoc times. Here it formed the basement to the Southern Uplands basin. Palaeontological evidence places this basin adjacent to Pomeroy, Co. Tyrone in the early Caradoc. Sinistral strike-slip faulting, from the late Ashgill transported the Southern Uplands Terrane to its present location, a distance of less than 250 km.

**Keywords:** Ballantrae Complex, Arenig chert, rare earth elements geochemistry.

Arenig terranes in the northern British Caledonides to the south of the Highland Border contain volcanics and deep water sediments which originated outboard of the Laurentian margin. These include the Ballantrae Complex, a highly tectonized Arenig ophiolite and, to the south of the Southern Upland Fault, lavas and cherts within the Leadhills Imbricate Zone which lies to the north of the Leadhills Fault (Fig. 1). The pre-deformation geological history of the Imbricate Zone rocks is currently unknown.

These Arenig rocks provide a window into the tectonic environments pertaining during a critical, pre-collisional phase in the evolution of the British Caledonides. In this paper we use chert rare earth element (REE) geochemistry of biostratigraphically well-constrained samples to reconstruct the original tectonic environments of these allochthonous, terranes and present a model for the tectonic setting and early collisional history of this part of the Laurentian margin.

### Ballantrae Complex

The Ballantrae Ophiolite Complex (Church & Gayer 1973; Bluck 1978) has played an important role in reconstruction of the plate configuration of the Caledonian Orogeny. The complex contains the components of an ophiolite which was thrust onto the Midland Valley microplate. Bluck *et al.* (1980) suggested that most of the volcanic rocks in the Ballantrae

Complex were generated in an island-arc marginal basin; a U–Pb zircon age of  $483 \pm 4$  Ma for a trondhjemite body dating the genesis of the ophiolite and a K–Ar age of  $478 \pm 4$  Ma on an amphibole in the metamorphic aureole, dating emplacement. The section at Bennane Head (locality Bennane Lea grid ref. [NX 09108610]; Lewis 1975; Stone & Smellie 1988; Bluck 1992b) exposes the Balcreuchan Group comprising volcanic and associated sedimentary rocks, including *c.* 30 m of red and green radiolarian chert (Fig. 2). The clastic sedimentary rocks within and underlying the pillow lavas contain graptolites, including *Tetragraptus fruticosus*, *Sigmagraptus praecursor*, *Didymograptus extensus* and *D. cf. protomurchisoni*, indicative of an early to mid-Arenig age (Stone & Rushton 1983). Intimately associated with the lavas and black and red cherts are fine volcanoclastic breccias and hyalotuffs, indicative of a shallow marine origin, together with black graptolitic mudstones (Bluck 1992b). Further to the north, near Balcreuchan Port, low Arenig graptolites, including the eponymous zonal index species *Tetragraptus approximatus*, have been found in red cherty mudstones (Stone & Rushton 1983). Both radiometric and biostratigraphical ages are consistent with the formation of the succession in early to mid-Arenig times.

The oldest part of the Ballantrae lava sequence contains rare prehnite, epidote and titanite as alteration products suggesting burial metamorphism to the prehnite-pumpellyite facies (Smellie 1984) and suggesting the possibility that the cherts in the succession may be recrystallized. However, the cherts show

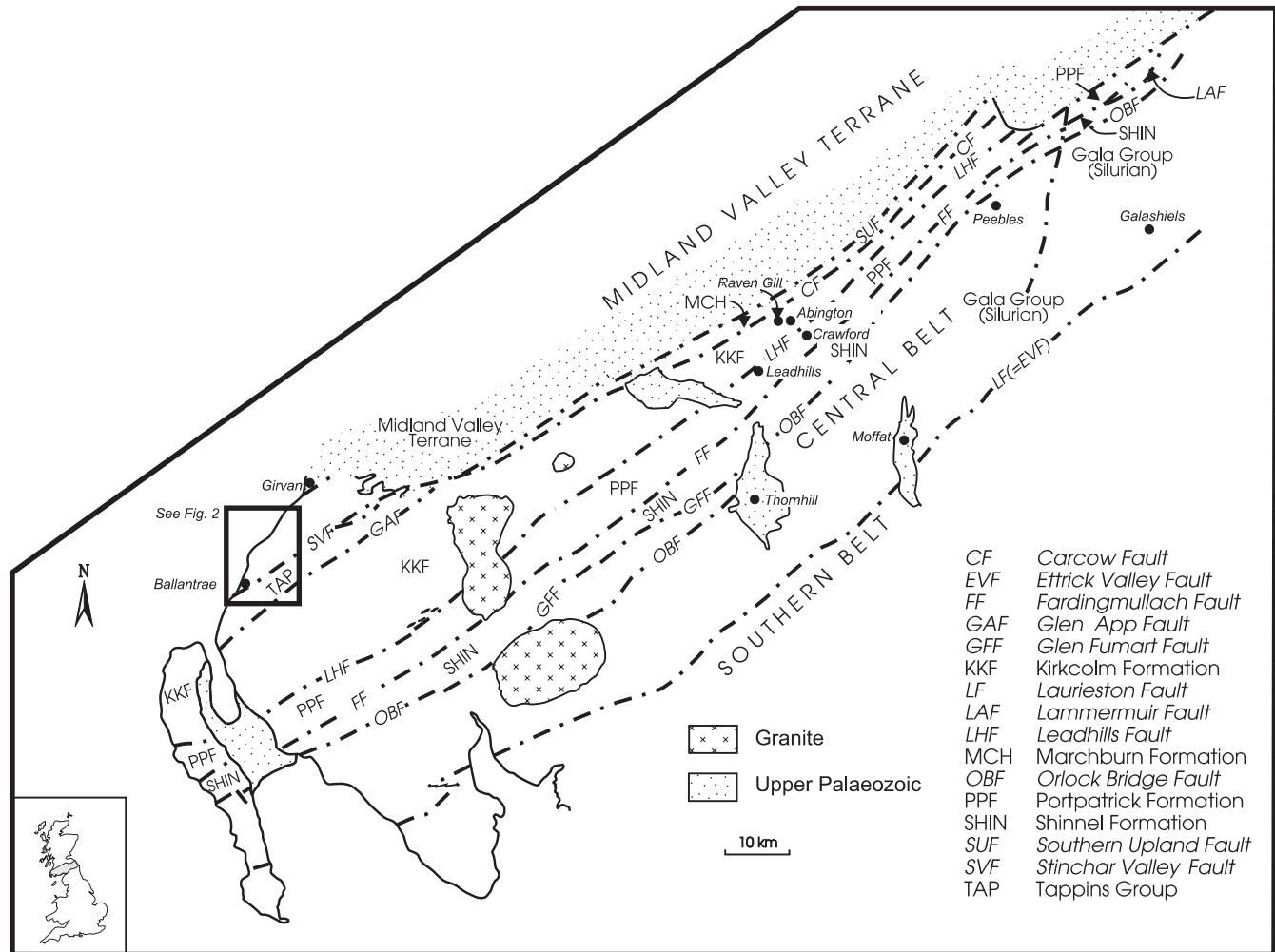


Fig. 1. General geological map of Southern Uplands and Ballantrae area (redrawn after Floyd 1996). The Leadhills Imbricate Zone lies to immediately to the north of the Leadhills Fault and extends across the Southern Uplands Terrane. The zone is only 1.8 km wide and cannot be illustrated at the scale of this map.

little visible evidence of recrystallization and contain well preserved radiolarians and conodonts (Aitchison 1998).

The lavas were generated in a variety of tectonic settings (Wilkinson & Cann 1974). Of specific interest to this study, the lavas (and associated cherts) from the southerly coastal outcrops at Bennane Lea (Bluck 1992b) have been attributed to an ocean island setting based on their trace element geochemistry (Wilkinson & Cann 1974; Jones 1977; Thirlwall & Bluck 1984; Fig. 2). Stone & Smellie (1990) and Bluck (1992b) considered this was close to a rifted island arc. Elsewhere in the complex, lavas of island-arc affinity are known from Games Loup and Mains Hill (Lewis 1975; Wilkinson & Cann 1974; Jones 1977; Thirlwall & Bluck 1984; Bluck 1992a; Fig. 2). Lewis & Bloxham (1977) recognized both island-arc and oceanic island lavas based on REE data. The southern margin of the complex is defined by the Stinchar Valley Fault, the western part of the Southern Upland Fault (Floyd 1994, 1996).

In a review of western Pacific and ancient ophiolites Searle & Stevens (1984) concluded that all are connected with short-lived, intra-oceanic subduction zones and marginal basins and island arcs in varying degrees of maturity. Using a uniformitarian approach, a number of hypotheses have been proposed to explain the geological evolution of the Ballantrae Complex.

Barrett *et al.* (1982) considered the ocean island lavas to represent an intra-plate volcanic edifice, seamount or plateau. Northward subduction beneath the Midland Valley caused the collision of the seamount with the trench, high level volcanics were accreted or obducted onto the continental margin basement (north of the Stinchar Valley Fault). This hypothesis ignored the existence of a volcanic arc and is rejected. They also suggested a period of northward subduction without accretion prior to the emplacement of the Downan Point Lava Formation in the mid-Ordovician. Though plausible, to have a period of some 30 Ma of subduction with apparently no geological evidence of accretion seems unlikely. The Downan Point Lava Formation could in part fill this stratigraphical gap but its age is poorly known. An imprecise Sm-Nd age date of  $468 \pm 22$  Ma was obtained by Thirlwall & Bluck (1984).

A more likely hypothesis for the origin of the Ballantrae Complex is a variation of the island-arc marginal basin model proposed by Bluck *et al.* (1980; see also Bluck 1992a) who envisaged an arc developed above a north-dipping subduction zone (Hypothesis a, Fig. 3a). Stone & Smellie (1990) and Smellie & Stone (1992) favoured an origin for the Ballantrae Complex in a back-arc basin above a south-dipping

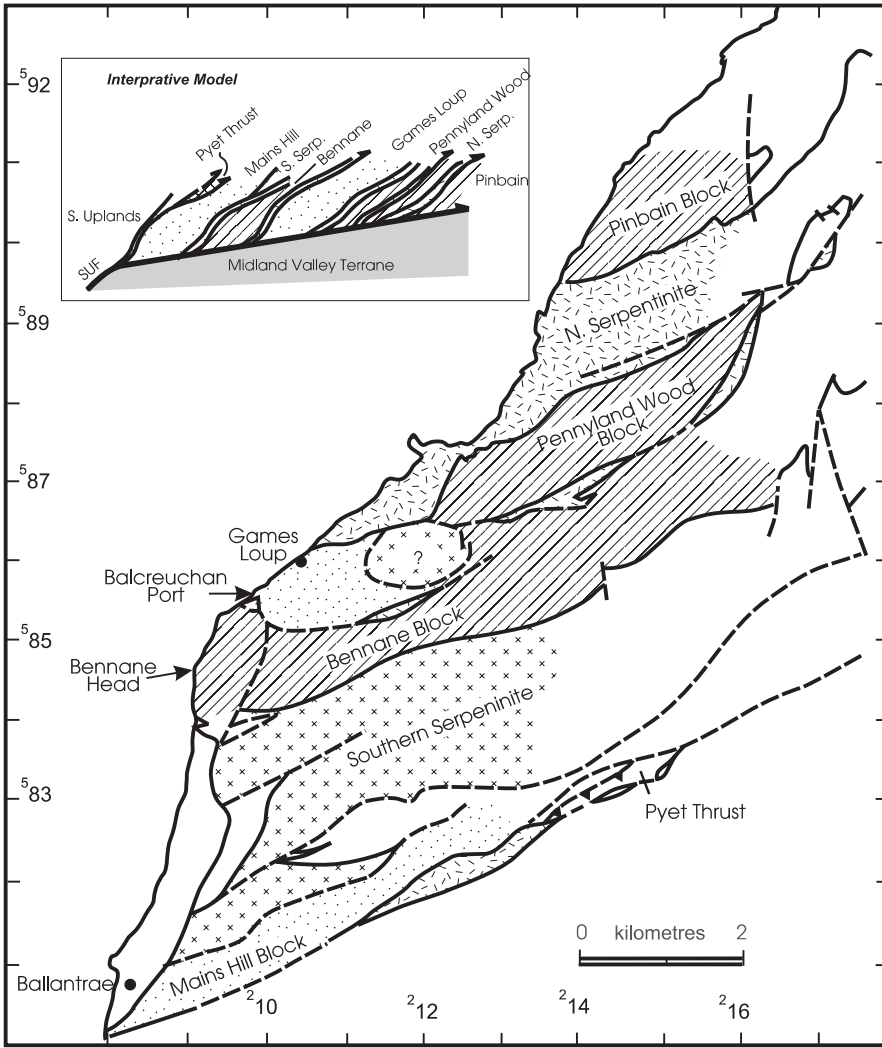


**Fig. 2.** Simplified tectonostratigraphic map of the Ballantrae Complex. The model cross-section represents the situation in the late Arenig. Ornament indicates the components of the complex with similar tectono-stratigraphic setting based upon published geochemical analyses. The Pinbain, Pennyland Wood and Bennane blocks are of ocean island affinity whilst the Mains Hill and Games Loup Blocks are of island arc affinity.

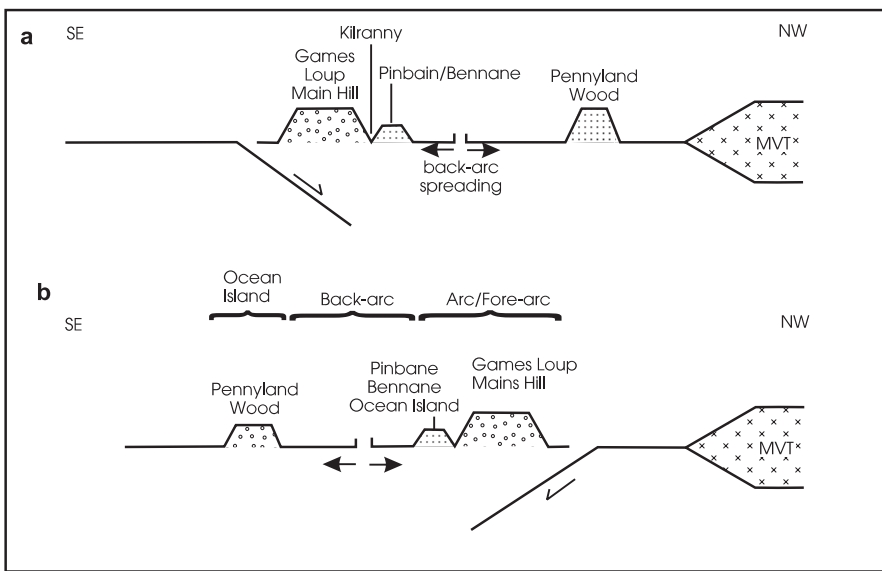


**Fig. 3.** Alternative hypotheses to explain the origin and emplacement of the Ballantrae Complex (redrawn after Stone & Smellie 1990, fig. 6).

subduction zone (Hypothesis b, Fig. 3b). They noted however (p. 543) that either a northwards or southwards subduction model could be applied to the complex, as both were consistent

with the known lithostratigraphical and geochemical constraints. Further, the complex was then tectonically telescoped during obduction and a reversal in subduction polarity.

In hypothesis a the cherts of the Ballantrae Complex formed in a basin close to the continental margin and should inherit the geochemical character of that margin. In hypothesis b the cherts would have been deposited within a back-arc basin or open ocean setting, separated from the continental margin by a trench. The trench would have trapped sediment destined for the basin and in this hypothesis cherts would inherit the geochemical character of the ocean. Elucidation of the depositional setting of these cherts thus provides a definitive test of these hypotheses.

### Leadhills Imbricate Zone

This zone extends as a 1.8 km wide zone to the immediate north of the Leadhills Fault (Fig. 1). It is one of the most complex parts of the Northern Belt in terms of the structure, formal definition of the stratigraphical units present and their distinction from those of the structural zone immediately to the north (Leggett *et al.* 1979). The zone contains numerous repetitions of volcanic rocks, cherts, black shales and greywackes (Hepworth 1981; Hepworth *et al.* 1982; Leggett 1978; Leggett & Casey 1982). At least some of the greywackes belong in the Kirkcolm Formation (=Abington Formation of Hepworth 1981 and Hepworth *et al.* 1982) and the black shales are assumed to represent parts of the Moffat Shale Group either beneath or within the Kirkcolm Formation.

In his review of Southern Uplands stratigraphy, Floyd (1996) formalized the dominantly volcanic and chert units of the Leadhills Imbricate Zone as the Raven Gill and Kirkton formations within what he termed the Crawford Group. The Raven Gill Formation was defined, following Hepworth (1981) and Hepworth *et al.* (1982), for the basaltic pillow lavas, basic sheets, brown mudstones and radiolarian cherts at the eponymous type locality. Floyd (1996, p. 157) noted the Arenig age of the conodonts from Raven Gill (*Oepikodus evae* Biozone—see also Löfgren 1978, p. 38; Armstrong *et al.* 1990). Floyd (1996, p. 157) expressed uncertainty as to the unequivocal recognition of the Raven Gill Formation elsewhere along the Leadhills Imbricate Zone and suggested that the formation name should only be applied to rocks of proven Arenig age. He followed Hepworth (1981) in assigning the extensive development of grey and red cherts, red and green siliceous mudstones and lavas in the Leadhills Imbricate Zone to the Kirkton Formation. Floyd (1996) provisionally designated the pipeline section near Abington described by Leggett (1978, see also Leggett & Casey 1982, pp. 383–386) as the type section for the Kirkton Formation and considered the red and green siliceous mudstones described by Hepworth (1981) in Glencaple Burn near the confluence of Raven Gill [NS 9252 1988] as a reference section in the type area. Other reference sections were designated further to the northeast.

The outcrops along the Glencaple Burn were examined and sampled during the present study and confirm the observations of Hepworth (1981). Conodonts (Sample HOA11 from grid ref. [NS9250 1980] in the BGS collection) identified in the siliceous mudstones in the Kirkton Formation reference section, include *Oepikodus evae* and *Paracordylodus gracilis* suggesting the lower part of the Arenig *O. evae* Biozone is present at this locality. Ethington & Austin's (1993) record of a specimen of *Pygodus* from a loose piece of red siliceous mudstones from this general vicinity, suggests the presence somewhere locally of a latest Llanvirn–earliest Caradoc *P. anserinus* Biozone fauna comparable to those of the structural

zones to the north of the Leadhills Imbricate Zone and in mudstones associated with cherts in Normangill Burn ([NS9730 2375]; Lamont & Lindström 1957; confirmed during this study). The exact tectonostratigraphical relationship of the Normangill rocks to the Arenig of the Leadhills Imbricate Zone is unclear due to poor exposure. The record of Arenig conodonts from the Leadhills Imbricate Zone in the headwaters of the Snar Water by Smith (1907) was confirmed during the present study in conjunction with the sampling of grey cherts from the thick chert and shale succession here. Basalts are reported from the locality (Borthwick 1993, p. 199) and there is also a thick sequence of greywackes of unknown age.

The rocks of the Leadhills Imbricate Zone are also well exposed on the hills above Crawford (see Leggett & Casey 1982, fig. 5) where the track leading to the radio mast and the adjacent fields show faulted repetitions of grey radiolarian chert, greywacke and, on higher parts of the track, igneous rocks, brown shales and red cherty mudstones. The last of these have yielded low to mid-Arenig conodonts of the *O. evae* Biozone (*sensu* Fortey *et al.* 1995) in the present study and in samples subsequently collected by J. D. Floyd with T. Danelian of Edinburgh University (Armstrong & Dean 1996).

Conodont bearing cherts and siliceous mudstones, which are unequivocally part of the Leadhills Imbricate Zone, belong in the low to mid-Arenig *O. evae* Biozone. This would suggest that the Kirkton Formation in its type area is synonymous with the Raven Gill Formation—the latter name having formal priority. Although sharing very similar lithological characteristics, the red siliceous mudstones and grey cherts with black mudstones which crop out in fault bounded tracts to the north of the Leadhills Imbricate Zone yield *P. anserinus* Biozone faunas (Armstrong *et al.* 1990; Owen *et al.* 1999) and are therefore significantly younger (latest Llanvirn–earliest Caradoc) than the revised Raven Gill Formation of the Leadhills Imbricate Zone. It may eventually be appropriate to establish a new lithostratigraphical name for the younger chert-bearing unit.

Based on the conodont and graptolite biostratigraphy, the Raven Gill Formation of the Southern Uplands correlates with the chert bearing succession of the Ballantrae Complex and deposition of these cherts predates the obduction of the ophiolite. In order to reconstruct late Arenig palaeogeography and tectonostratigraphy the relationship between the rocks of the Leadhills Imbricate Zone and the Ballantrae Complex must be known.

### REE geochemistry and radiolarian chert depositional environment

Modern radiolarian oozes accumulate in a restricted range of depositional settings where nutrient-rich upwelling zones lead to high planktonic productivity (Hesse 1988). Ordovician to Cretaceous radiolarian cherts are also thought to have accumulated in high-latitude east–west upwelling belts and in continental margin zones (Jones & Murchev 1986, p. 467). Murray *et al.* (1991, 1992) have shown that the variation in REE composition in marine cherts and mudrocks results from a combination of (1) the composition of contained terrigenous particles, (2) the composition of contained metalliferous particles and (3) adsorption from sea water. As a result of the last of these, the total REE abundance is controlled by sediment exposure time (i.e. burial rate).



During the early diagenesis of cherts there is considerable chemical fractionation, notably the addition of dissolved silica, but Al, Ti and Fe and the REEs are immobile (Murray 1994). Murray (1994) convincingly demonstrated that while Al, Ti and Fe (expressed as oxides) can provide some discrimination between continental margin and proximal ridge settings, the REEs enable a further distinction to be made between proximal ridge and pelagic deposits (see also Girty *et al.* 1996). Murray *et al.* (1992) noted that the REE composition of chert records the interplay between terrigenous sources and scavenging from local seawater. Using shale-normalized REE patterns, total abundances,  $Ce_{anom}$  and La/Yb they were able to discriminate between oceanic (Pacific-type), large ocean basin surrounded by passive margins (Atlantic-type) and continental-margin cherts receiving large amounts of terrigenous material (Southern High Latitude (SHL)-type). Owen *et al.* (1999) have extended the application of chert REE geochemistry to the elucidation of the depositional setting of tectonized cherts within the Caledonian orogenic belt.

### Samples and analytical procedures

Cherts have been sampled from Bennane Lea and through the Leadhills Imbricate Zone (Table 1 for grid references). XRD analysis was used to provide a semi-quantitative assessment of non-silica components of the cherts and cherty shales and thus a purity check prior to ICP-MS analysis of the samples. Samples which did not fully enter into solution following reaction with hot Aristar hydrofluoric and nitric acids were excluded from the analysis. The ICP-MS analysis was undertaken on a Perkin Elmer Sciex Elan 6000 machine at the Department of Geological Sciences, University of Durham, calibrated using matrix-matched standards and an internal Rh standard was added to the samples prior to dilution. The limit of detection is  $3\sigma$  of the blanks and in all cases is  $<7$  ppb. The limit of quantification is  $10\sigma$  of the blanks and in all cases is  $<13$  ppb as shown by replicate analysis of the USGS reference rock standards SCo-1, W2, BCR1, BHVO1, RGM1 and x108 an internal laboratory quality control standard. Data points on the normalized REE plots have been scaled to include this error. All analysed samples contain microveins of quartz and/or calcite and the inclusion of some of this material was inevitable in virtually all of the powders for REE analysis. The consistency of REE patterns within and between the sample sets and in comparison with DSDP and ODP published data (Murray *et al.* 1992) confirm that any REE input from these veins is negligible.

A chondrite-normalized average REE pattern is likely to parallel the primordial abundances in the solar nebula and bulk Earth abundances. The values adopted here are for CI carbonaceous chondrites (Boynton 1984; values in Table 1). To enable comparison with other REE analyses of cherts, the ICP-MS results were also normalized against mean shale (see Murray 1994; Murray *et al.* 1990, 1991, 1992; values in Table 1), a technique also applied in seawater chemistry (e.g. Elderfield & Greaves 1982).

In addition to the shale and chondrite-normalized REE plots showing the overall REE patterns, normalized  $Ce_{anom}$ ,  $Eu_{anom}$  and La/Yb element ratios have been considered useful discriminants between samples and between plate tectonic environments (Murray *et al.* 1992; Owen *et al.* 1999). The  $Ce_{anom}$  and  $Eu_{anom}$  are calculated as recommended by Murray *et al.* (1992). These signatures seem to be robust despite considerable discussion in the literature of potential variation in cerium and possibly europium anomalies as a function of oceanic redox conditions (Wilde *et al.* 1996; Holser 1997). The degree of LREE v. HREE enrichment is assessed through the ratio of shale-normalized (sn) and chondrite-normalized (cn) La and Yb values,  $La_{sn}/Yb_{sn}$  and  $La_{cn}/Yb_{cn}$  respectively.

Radiolarian cherts deposited in a continental margin setting have essentially flat shale-normalized REE patterns, lacking the distinct negative  $Ce_{anom}$  characteristic of open ocean and mid-ocean ridge environments. The chondrite-normalized patterns show LREE enrich-

ment and inherited negative  $Eu_{anom}$ ,  $Ce_{anom} \approx 1$  and  $La_{sn}/Yb_{sn}$  values of  $\approx 1.2$ . A chondrite-normalized, negative  $Eu_{anom}$  typifies sediments from continental margin settings except where there is a significant input of detritus from undifferentiated igneous sources (McLennan *et al.* 1990). The latter sediments, rich in andesitic debris, have very slight or no such anomalies. Taylor & McLennan (1985) recognized that the absence of a negative  $Eu_{anom}$  in post-Archaeon sedimentary rocks is largely restricted to first-cycle volcanogenic sequences.

Chert REE patterns from open ocean settings, distant from the effects of terrigenous detrital input, are dominated by adsorption of dissolved REEs from seawater,  $Ce_{anom} \ll 1$  and  $La_{sn}/Yb_{sn} \approx 0.8-1$  as a result of the Ce-depleted seawater and preferential adsorption of LREEs from seawater (e.g.  $La_{sn}/Yb_{sn} \approx 0.4$ ), which increases the  $La_{sn}/Yb_{sn}$  ratio recorded in chert (Murray *et al.* 1992).

### Results

Raw REE abundances (in ppm) and chondrite and shale-normalized discriminates are tabulated in Table 1. Bennane Lea and Leadhills Imbricate Zone cherts can be characterized based on REE patterns,  $Ce_{anom}$ ,  $Eu_{anom}$  and to a lesser extent La/Yb.

The red and green radiolarian cherts from the bedded chert succession in the Ballantrae Complex at Bennane Lea (AOW1-6; Fig. 4a) have chondrite-normalized REE plots which show LREE enrichment, a Ce peak and a distinct Eu trough. Chondrite-normalized  $Ce_{anom}$  values range from 1.44 to 1.7 and  $Eu_{anom}$  from 0.70 to 0.79. The shale-normalized patterns are essentially flat with a distinct Ce peak reflecting a high, positive  $Ce_{anom}$  (1.51–1.78).  $Eu_{anom}$  values range from 1.05 to 1.33.  $La_{sn}/Yb_{sn}$  and  $La_{cn}/Yb_{cn}$  values range from 0.97 to 1.41 and 7.78 to 11.4 respectively. The XRD traces show only minor amounts of clays in addition to the quartz peaks and XRF data (Table 2) show higher MnO concentrations than in cherts from the Southern Uplands (Owen & Armstrong 1997, appendix 9) but values are still very low (0.25%).

A black radiolarian chert (AOW12; Fig. 4a) from the edge of the rudite outcrop to the immediate south of the bedded cherts at Bennane Lea lacks the Ce peak and is relatively depleted in chondrite-normalized LREEs compared to the red and green cherts AWO 1–6 (La/Sm 2.25 cf. 2.92–3.61). Significantly, the chondrite-normalized plot shows that there is virtually no  $Eu_{anom}$  (0.88) in the black chert suggesting the presence of a component derived from an immature arc (McLennan *et al.* 1990). However both XRD and XRF show sample AOW12 to be almost pure silica.  $La_{sn}/Yb_{sn}$  and  $La_{cn}/Yb_{cn}$  values are also low for this sample at 0.57 and 4.19 respectively.

Leadhills Imbricate Zone cherts show typical continental margin REE patterns (Fig. 4b), have chondrite-normalized  $Ce_{anom}$  values which range from 0.9 to 1.21 and  $Eu_{anom}$  from 0.61 to 0.79. Shale-normalized  $Ce_{anom}$  values range from 0.95 to 1.23 and  $Eu_{anom}$  from 0.86 to 1.13.  $La_{sn}/Yb_{sn}$  and  $La_{cn}/Yb_{cn}$  for cherts have values of 0.95 (0.46 for sample AWO1)–1.27 and 4.92 (3.48 for sample AWO1)–13.88.

### Interpretation

Murray *et al.* (1990) obtained a sequence of shale-normalized  $Ce_{anom}$  values for the Franciscan Complex of California ranging from extremely low values (about 0.29) for cherts and shales deposited near the spreading ridge, through values around 0.55 for those deposited in ocean basin settings

Table 1. Rare earth element data

| Grid ref.            | AOW1<br>NX091861 | AOW2<br>NX091861 | AOW3<br>NX091861 | AOW4<br>NX091861 | AOW5<br>NX091861 | AOW6<br>NX091861 | AOW12<br>NS922214 | AOW36<br>NS922214 | AOW58<br>NS922214 | AOW59<br>NS922214 | AOW62<br>NS922214 | AOW63<br>NS922214 | AOW64<br>NS922214 | AOW65<br>NS922214 | AOW67<br>NS922214 | AOW68<br>NS922214 | AOW69<br>NS922214 | AOW73<br>NS922214 | AOW1<br>NS922214 | AOW6<br>NS922214 | AOW7<br>NS922214 | AOW8<br>NS922214 |  |
|----------------------|------------------|------------------|------------------|------------------|------------------|------------------|-------------------|-------------------|-------------------|-------------------|-------------------|-------------------|-------------------|-------------------|-------------------|-------------------|-------------------|-------------------|------------------|------------------|------------------|------------------|--|
| Raw (ppm)            |                  |                  |                  |                  |                  |                  |                   |                   |                   |                   |                   |                   |                   |                   |                   |                   |                   |                   |                  |                  |                  |                  |  |
| La                   | 41               | 14.336           | 6.324            | 9.664            | 8.853            | 18.14            | 3.154             | 16.44             | 18.42             | 15.25             | 2.84              | 6.11              | 44.19             | 17.09             | 9.85              | 13.24             | 8.27              | 5.81              | 4.80             | 9.91             | 13.69            | 7.39             |  |
| Ce                   | 0.81             | 83.10            | 19.88            | 30.63            | 27.70            | 54.79            | 6.22              | 32.37             | 41.25             | 35.52             | 5.77              | 13.40             | 93.22             | 42.81             | 24.60             | 26.92             | 19.58             | 11.53             | 12.33            | 21.27            | 29.53            | 13.66            |  |
| Pr                   | 0.12             | 10.10            | 3.41             | 2.34             | 2.20             | 4.34             | 0.81              | 4.04              | 4.12              | 3.61              | 0.67              | 1.50              | 10.70             | 3.96              | 2.69              | 2.85              | 1.83              | 1.48              | 1.26             | 2.21             | 2.95             | 1.67             |  |
| Nd                   | 0.60             | 38.30            | 13.94            | 6.39             | 8.63             | 17.86            | 3.57              | 16.17             | 15.70             | 13.58             | 2.64              | 5.87              | 42.78             | 15.19             | 10.98             | 11.25             | 7.42              | 6.13              | 5.60             | 9.47             | 12.45            | 7.27             |  |
| Sm                   | 0.20             | 7.50             | 2.86             | 1.36             | 1.72             | 3.74             | 0.88              | 3.49              | 2.73              | 2.50              | 0.48              | 1.12              | 8.38              | 2.90              | 2.39              | 2.25              | 1.50              | 1.23              | 1.18             | 1.91             | 2.41             | 1.36             |  |
| Eu                   | 0.07             | 1.61             | 0.67             | 0.40             | 0.39             | 0.89             | 0.26              | 0.78              | 0.54              | 0.47              | 0.13              | 0.28              | 1.80              | 0.61              | 0.49              | 0.46              | 0.33              | 0.28              | 0.26             | 0.40             | 0.51             | 0.29             |  |
| Gd                   | 0.26             | 6.51             | 2.81             | 1.39             | 1.66             | 3.70             | 0.91              | 3.45              | 2.26              | 2.08              | 0.48              | 1.10              | 2.59              | 0.99              | 0.78              | 0.78              | 0.56              | 0.43              | 0.43             | 0.62             | 0.82             | 0.41             |  |
| Tb                   | 0.05             | 1.23             | 0.39             | 0.21             | 0.24             | 0.54             | 0.16              | 0.48              | 0.33              | 0.30              | 0.07              | 0.16              | 0.78              | 0.25              | 0.22              | 0.22              | 0.15              | 0.15              | 0.22             | 0.25             | 0.31             | 0.19             |  |
| Dy                   | 0.32             | 6.51             | 2.10             | 1.18             | 1.33             | 3.07             | 1.00              | 2.66              | 1.70              | 1.66              | 0.43              | 0.96              | 6.78              | 2.00              | 2.29              | 2.38              | 1.57              | 1.12              | 1.38             | 1.42             | 1.83             | 1.11             |  |
| Ho                   | 0.07             | 1.34             | 0.42             | 0.22             | 0.29             | 0.63             | 0.21              | 0.52              | 0.35              | 0.34              | 0.08              | 0.19              | 1.39              | 0.39              | 0.49              | 0.52              | 0.34              | 0.23              | 0.29             | 0.29             | 0.36             | 0.23             |  |
| Er                   | 0.21             | 3.75             | 1.04             | 0.59             | 0.79             | 1.68             | 0.57              | 1.38              | 0.93              | 0.88              | 0.24              | 0.52              | 3.71              | 1.09              | 1.35              | 1.43              | 0.91              | 0.60              | 0.84             | 0.86             | 0.98             | 0.63             |  |
| Tm                   | 0.03             | 0.53             | 0.16             | 0.10             | 0.12             | 0.27             | 0.09              | 0.20              | 0.15              | 0.15              | 0.04              | 0.08              | 0.58              | 0.17              | 0.22              | 0.22              | 0.14              | 0.09              | 0.14             | 0.14             | 0.17             | 0.11             |  |
| Yb                   | 0.21             | 3.53             | 0.92             | 0.54             | 0.59             | 1.57             | 0.51              | 1.22              | 0.90              | 0.89              | 0.23              | 0.53              | 3.50              | 1.07              | 1.35              | 1.30              | 0.88              | 0.56              | 0.93             | 0.90             | 1.12             | 0.66             |  |
| Lu                   | 0.03             | 0.53             | 0.14             | 0.08             | 0.10             | 0.25             | 0.08              | 0.19              | 0.14              | 0.14              | 0.04              | 0.08              | 0.55              | 0.17              | 0.21              | 0.20              | 0.14              | 0.09              | 0.15             | 0.16             | 0.18             | 0.11             |  |
| Chondrite normalized |                  |                  |                  |                  |                  |                  |                   |                   |                   |                   |                   |                   |                   |                   |                   |                   |                   |                   |                  |                  |                  |                  |  |
| Ce*                  | 37.10            | 16.62            | 25.65            | 24.52            | 22.69            | 47.02            | 8.40              | 43.09             | 46.61             | 39.38             | 7.34              | 15.99             | 115.13            | 43.79             | 26.93             | 33.05             | 20.83             | 15.45             | 12.89            | 25.05            | 34.17            | 18.78            |  |
| Ce/Ce*               | 1.70             | 1.48             | 1.48             | 1.44             | 1.51             | 1.44             | 0.92              | 0.93              | 1.10              | 1.12              | 0.97              | 1.04              | 1.00              | 1.21              | 1.13              | 1.01              | 1.16              | 0.92              | 1.18             | 1.05             | 1.07             | 0.90             |  |
| Sm/Nd                | 0.63             | 0.66             | 0.58             | 0.61             | 0.61             | 0.64             | 0.76              | 0.66              | 0.53              | 0.57              | 0.56              | 0.59              | 0.60              | 0.59              | 0.67              | 0.62              | 0.62              | 0.65              | 0.62             | 0.62             | 0.59             | 0.57             |  |
| Eu*                  | 12.75            | 6.18             | 7.59             | 7.61             | 7.20             | 16.73            | 4.01              | 15.61             | 11.91             | 10.77             | 2.17              | 5.00              | 36.72             | 12.43             | 10.86             | 10.15             | 6.84              | 5.64              | 5.46             | 8.41             | 10.62            | 5.96             |  |
| Eu/Eu*               | 0.72             | 0.79             | 0.72             | 0.70             | 0.72             | 0.72             | 0.88              | 0.68              | 0.62              | 0.60              | 0.79              | 0.75              | 0.67              | 0.67              | 0.61              | 0.62              | 0.65              | 0.66              | 0.65             | 0.65             | 0.66             | 0.67             |  |
| Ce/La                | 1.36             | 1.21             | 1.18             | 1.14             | 1.20             | 1.16             | 0.76              | 0.76              | 0.86              | 0.89              | 0.78              | 0.84              | 0.81              | 0.96              | 0.96              | 0.78              | 0.91              | 0.76              | 0.99             | 0.82             | 0.83             | 0.71             |  |
| La/Sm                | 3.16             | 2.92             | 3.61             | 3.51             | 3.44             | 3.05             | 2.25              | 2.96              | 4.25              | 3.84              | 3.71              | 3.43              | 3.32              | 3.71              | 2.59              | 3.70              | 3.48              | 2.97              | 2.56             | 3.26             | 3.58             | 3.42             |  |
| Gd/Yb                | 2.47             | 2.08             | 2.23             | 1.82             | 2.09             | 1.90             | 1.44              | 2.28              | 2.30              | 2.05              | 1.72              | 1.69              | 1.82              | 1.95              | 1.46              | 1.41              | 1.43              | 1.85              | 1.09             | 1.62             | 1.66             | 1.58             |  |
| La/Yb                | 10.53            | 7.88             | 11.44            | 8.84             | 9.78             | 7.78             | 4.19              | 9.07              | 13.88             | 11.57             | 8.44              | 7.84              | 8.52              | 10.76             | 4.92              | 6.88              | 6.34              | 6.99              | 3.48             | 7.40             | 8.26             | 7.59             |  |
| Shale normalized     |                  |                  |                  |                  |                  |                  |                   |                   |                   |                   |                   |                   |                   |                   |                   |                   |                   |                   |                  |                  |                  |                  |  |
| Ce*                  | 0.34             | 0.15             | 0.24             | 0.23             | 0.21             | 0.44             | 0.08              | 0.40              | 0.43              | 0.36              | 0.07              | 0.15              | 1.07              | 0.40              | 0.25              | 0.30              | 0.19              | 0.14              | 0.12             | 0.23             | 0.31             | 0.17             |  |
| Ce/Ce*               | 1.78             | 1.55             | 1.55             | 1.52             | 1.59             | 1.51             | 0.95              | 0.97              | 1.16              | 1.17              | 1.02              | 1.09              | 1.05              | 1.27              | 1.17              | 1.07              | 1.23              | 0.96              | 1.23             | 1.11             | 1.14             | 0.95             |  |
| Eu*                  | 0.37             | 0.17             | 0.24             | 0.23             | 0.22             | 0.47             | 0.10              | 0.50              | 0.38              | 0.34              | 0.07              | 0.16              | 1.16              | 0.39              | 0.35              | 0.32              | 0.22              | 0.18              | 0.18             | 0.27             | 0.34             | 0.19             |  |
| Eu/Eu*               | 1.14             | 1.33             | 1.05             | 1.05             | 1.09             | 1.17             | 1.65              | 0.97              | 0.89              | 0.86              | 1.13              | 1.07              | 0.96              | 0.96              | 0.87              | 0.89              | 0.92              | 0.94              | 0.92             | 0.93             | 0.94             | 0.96             |  |
| La/Yb                | 1.34             | 1.00             | 1.41             | 1.05             | 1.29             | 0.97             | 0.57              | 1.11              | 2                 | 1.72              | 1.16              | 1.06              | 1.13              | 1.73              | 0.78              | 0.86              | 0.96              | 0.87              | 0.46             | 1.41             | 1.03             | 0.94             |  |

Normalized cerium (Ce/Ce\*) and europium (Eu/Eu\*) anomalies were calculated as recommended by (inter alia) Murray et al. (1992) as follows:  
 $Ce^{anom} = Ce^{normalized}/Ce^*$  where  $Ce^* = (La^{normalized} + Pr^{normalized})/2$  and  $Eu^{anom} = Eu^{normalized}/Eu^*$  where  $Eu^* = (Sm^{normalized} + Gd^{normalized})/2$ . Samples AOW 1–12 are from Benmaine Lea [NX 0910 8610]. Samples AOW 36 [Crawford Track NS 942 214]; AOW 58, 59, 62–65 [Glencaple Burn NS 922 214]; AOW1, AOW 67–69 [Raven Gill NS 925 198]; AOW 6–7, AOW 73 [Snar Water NS 871 154] are from the Raven Gill Formation in the Southern Uplands.

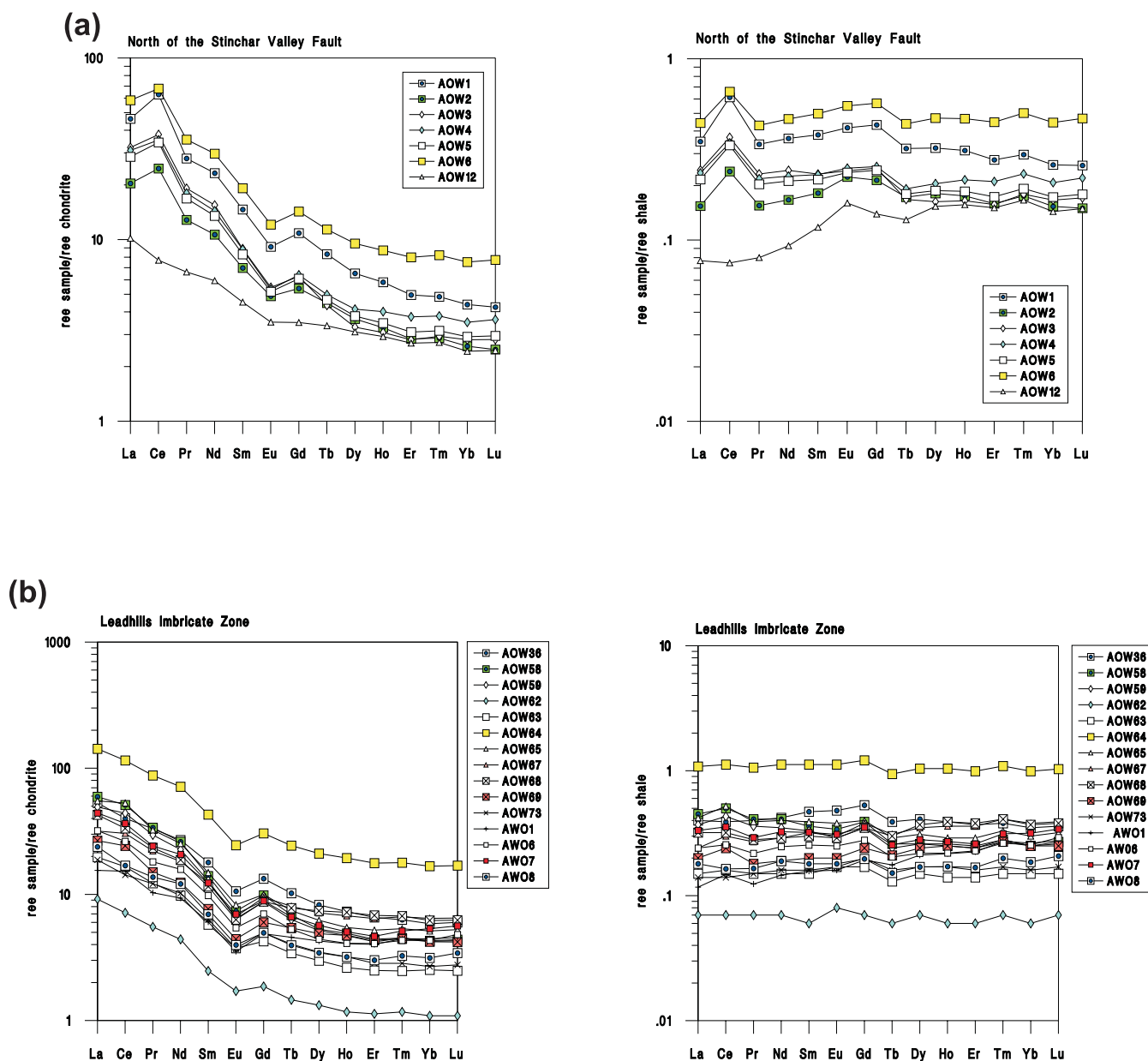


Fig. 4. Chondrite- and shale-normalized REE plots for Arenig cherts from Ballantrae and the Leadhills Imbricate Zone. (a) Plots of the Bennane Lea data. (b) Plots of the Raven Gill Formation chert data.

and 0.90–1.30 for cherts and shales from continental margin settings estimated to be over 3000 km from the spreading ridge.

Taking a larger data set, derived from DSDP and ODP cores from several oceans, Murray *et al.* (1992) were able to define four groups of cherts based upon REE geochemistry. Their raw data are chondrite-normalized herein using the values of Boynton (1984) to facilitate comparison (Fig. 5, Table 3). Pacific Ocean cherts typify a depositional setting far removed from significant terrigenous input. These cherts record a REE pattern dominated by adsorption of dissolved REEs from seawater. Cherts from the Atlantic basin, a moderate-sized basin surrounded by passive margins and a higher terrigenous input record a mixture of adsorbed and terrigenous input, with moderately negative shale-normalized  $Ce_{anom}$  and  $La_{sn}/Yb_{sn}$  intermediate to those of Pacific type and

terrigenous input. Cherts from Southern High Latitudes (SHL), a region dominated by large terrigenous input from the Antarctic passive margin with inherited shale-normalized  $Ce_{anom}$  and  $Eu_{anom}$  values show chondrite-normalized  $Ce_{anom}$  values are the highest for the dataset. Chondrite-normalized  $Eu_{anom}$  values are the lowest for the dataset, and  $La_{sn}/Yb_{sn}$  and  $La_{cn}/Yb_{cn}$  values are the highest for the dataset reflecting the marked LREE enrichment in terrigenous detritus. Indian Ocean cherts are intermediate between those of Pacific and Atlantic-type.

Normalized  $Ce_{anom}$  and  $Eu_{anom}$  values in Bennane Lea cherts indicate the dominant nature of the terrigenous input. Normalized  $La/Yb$  values are typical for either Atlantic or Indian Ocean-type cherts. The positive  $Ce_{anom}$  is unusual. A single sample (27-260-10) from the Gascoyne Abyssal Plain (Leg 27, Hole 260; 16°08.67'S, 110°17.92'E), between the

**Table 2.** Major and trace element data for selected cherts

|                                | AOW2   | AOW3  | AOW4   | AOW5  | AOW6  | AOW12 |
|--------------------------------|--------|-------|--------|-------|-------|-------|
| Major elements (%)             |        |       |        |       |       |       |
| SiO <sub>2</sub>               | 93.29  | 90.89 | 91.74  | 90.9  | 77.41 | 97.62 |
| Al <sub>2</sub> O <sub>3</sub> | 1.8    | 2.82  | 2.86   | 2.47  | 5.87  | 0.59  |
| Fe <sub>2</sub> O <sub>3</sub> | 1.74   | 2.87  | 3.19   | 2.98  | 8.44  | 0.26  |
| MgO <sup>-</sup>               | 0.79   | 0.65  | 0.62   | 0.8   | 1.76  | 0.15  |
| CaO                            | 1.72   | 0.31  | 0.11   | 0.68  | 0.87  | 0.67  |
| Na <sub>2</sub> O              | 0.36   | 0.25  | 0.54   | 0.29  | 0.91  | 0.16  |
| K <sub>2</sub> O               | 0.5    | 0.91  | 0.74   | 0.69  | 1.78  | 0.17  |
| TiO <sub>2</sub>               | 0.1    | 0.2   | 0.17   | 0.16  | 0.52  | 0.06  |
| MnO                            | 0.18   | 0.14  | 0.1    | 0.13  | 0.25  | 0.02  |
| P <sub>2</sub> O <sub>5</sub>  | 0.04   | 0.04  | 0.04   | 0.06  | 0.15  | 0.26  |
| Total                          | 100.52 | 99.07 | 100.11 | 99.15 | 97.94 | 99.96 |
| Al+Fe                          | 3.54   | 5.69  | 6.05   | 5.45  | 14.31 | 0.85  |
| Al/Al+Fe                       | 0.51   | 0.5   | 0.47   | 0.45  | 0.41  | 0.69  |
| Trace elements (ppm)           |        |       |        |       |       |       |
| Nb                             | 2.8    | 4.5   | 4      | 2.5   | 7     | 3.4   |
| Zr                             | 16.7   | 31.2  | 27.5   | 25.6  | 69    | 5.2   |
| Y                              | 10.9   | 8.6   | 10.4   | 8.6   | 15.1  | 10.7  |
| Sr                             | 28.8   | 35.5  | 37.8   | 43.3  | 46.9  | 42    |
| U                              | 0.5    | 1.9   | 0.5    | 10    | -1.1  | 2.6   |
| Th                             | 0.2    | 4.5   | 2.8    | 1     | 5.7   | 0     |
| Pb                             | 11.4   | 6.1   | 7.5    | 6.1   | 11.5  | 4.1   |
| Ga                             | 4.6    | 5.7   | 0.4    | 4.6   | 6.6   | 0.7   |
| Zn                             | 14.1   | 32.7  | 39.8   | 31.8  | 58.1  | 7.9   |
| Cu                             | 9.7    | 7.6   | 11.8   | 11.3  | 19    | 55.2  |
| Ni                             | 15.6   | 19.7  | 28.5   | 17    | 81.4  | 14.8  |
| Co                             | 9.4    | 12.2  | 26.4   | 24.9  | 34.6  | 5.1   |
| Cr                             | 12.5   | 25.6  | 25.9   | 21.2  | 327.1 | 25.2  |
| V                              | 35.1   | 52.6  | 45.4   | 44.8  | 98    | 49.1  |
| Rb                             | 15.6   | 32    | 23.5   | 23.2  | 54.3  | 3.1   |
| Ba                             | 282.7  | 161.2 | 148.7  | 343.7 | 246.3 | 134.6 |
| Ce                             | 19.3   | 34.6  | 33.3   | 27.3  | 81.9  | 3.3   |
| Nd                             | 7.3    | 7.1   | 7      | 5.7   | 19.5  | 4.9   |
| La                             | 9.1    | 10.9  | 11.7   | 11.2  | 25    | 4.5   |
| Sc                             | 1.8    | 2.9   | 1.8    | 3.1   | 9.5   | 1     |
| Ce/La                          | 2.12   | 3.17  | 2.85   | 2.44  | 3.28  | 0.73  |

Analysed by XRF following standard techniques. Sample localities as in Table 1.

Australian passive margin and the Java trench, has a REE pattern identical to that of the red and green cherts from Bennane Lea, including positive Ce<sub>anom</sub> (Murray *et al.* 1992; Table 3). This environment is consistent with the Tethyan-type ophiolite in so far as it formed in a marginal basin between a continental margin and a trench.

Cherts from the Leadhills Imbricate Zone have Ce<sub>anom</sub> and Eu<sub>anom</sub> values which are similar to those of Southern High Latitude cherts and normalized La/Yb values comparable to either Atlantic- or SHL-type cherts. On balance the Leadhills data compare most closely with those of cherts from Southern High Latitudes. This indicates a basinal setting close to the continental margin and a REE geochemistry dominated by terrigenous detritus. It is concluded that the cherts from the Leadhills Imbricate Zone accumulated closer to the continental margin than those from the Ballantrae Complex.

### Terrane analysis

Our chert REE data indicate that the Ballantrae marginal basin was receiving clastic material from a nearby continental margin. This conclusion supports the model, proposed by Stone & Smellie (1990) and Bluck (1992*b*), that the Ballantrae Complex developed in a rifted back-arc setting above a northward dipping subduction zone (hypothesis a Fig. 3).

Similarly the cherts of the Leadhills Imbricate Zone formed close to a continental margin. By analogy with modern collisional margins the Leadhills Imbricate Zone could therefore represent: (1) a fragment of the proximal part of a marginal basin trapped and deformed during obduction, (2) a sliver of allochthonous Arenig rocks emplaced during post-obduction, strike-slip faulting, or (3) an accreted fragment of oceanic crust (rejected following arguments in Armstrong *et al.* 1996 and the continental margin REE patterns presented herein). The tectonostratigraphical relationship between the Ballantrae Complex and unequivocal Arenig rocks of the Leadhills Imbricate Zone (Raven Gill Formation) helps constrain the nature of the southern margin of the Midland Valley terrane during the Arenig, the early history of the Southern Upland Fault and its status as a terrane boundary. If the Ballantrae Complex was emplaced over the Leadhills Imbricate Zone succession then one might envisage a scenario in which the conversion of a pre-Arenig mid-ocean ridge-fracture zone system into a subduction zone-arc system was followed by northward emplacement of the ophiolite as elements in the marginal basin became trapped at the subduction zone (cf. the model proposed by Dewey & Shackleton (1984) for the ophiolites of the Grampian tract). Alternatively the Ballantrae Complex may have been emplaced prior to the juxtaposition of the Southern Uplands and Midland Valley Terranes, in which



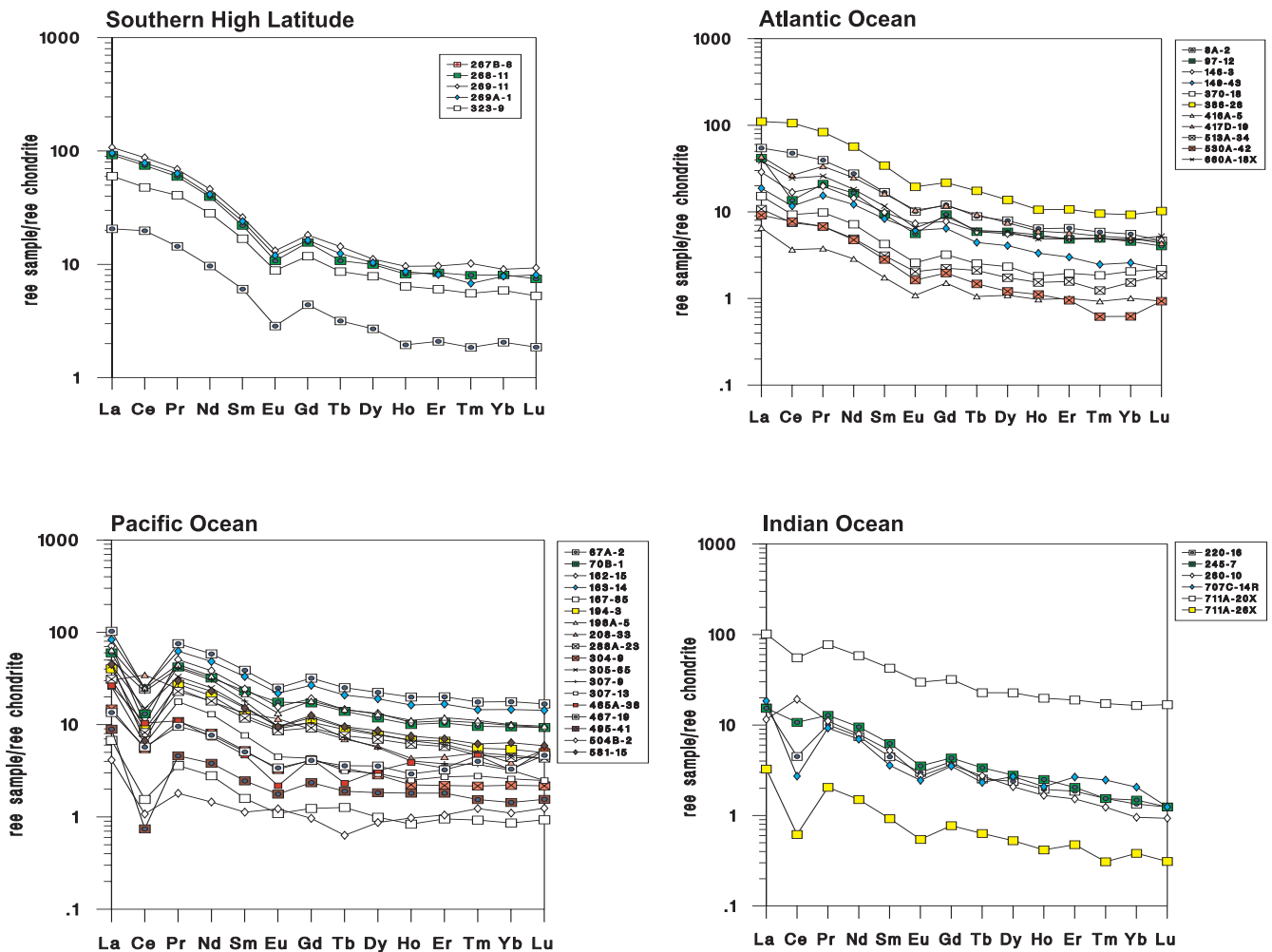


Fig. 5. Chondrite-normalized REE plots plotted from ODP and DSDP data collected by Murray *et al.* (1992). Chondrite normalization follows the method used herein to allow direct comparison of the datasets.

Table 3. Comparison of REE discriminants calculated from ODP and DSDP data compiled by Murray *et al.* (1992)

| Setting       |   | Ce <sub>anom</sub><br>shale     | Eu <sub>anom</sub><br>shale | La <sub>sn</sub> /Yb <sub>sn</sub> | Ce <sub>anom</sub><br>chondrite | Eu <sub>anom</sub><br>chondrite | La <sub>cn</sub> /Yb <sub>cn</sub> |
|---------------|---|---------------------------------|-----------------------------|------------------------------------|---------------------------------|---------------------------------|------------------------------------|
| Pacific-type  | Far removed from terrigenous input                    | ≤ 1<br>0.12–1.69 clusters @ 0.5 | 0.97–1.23                   | 0.8–1                              | 0.11–0.51                       | 0.67–1.17                       | 3.75–7.87                          |
| Atlantic-type | Moderate-sized basin surrounded by passive margins    | 0.19–0.61                       | 0.97–1.63                   | 0.82–1.86                          | 0.68–1.01                       | 0.68–0.83                       | 6.0–14.68                          |
| SHL-type      | Large terrigenous input from Antarctic passive margin | c. 1                            | c. 0.8                      | 1.27–1.45                          | 0.95–1.13                       | 0.55–0.62                       | 10–12.25                           |

Indian Ocean cherts have values intermediate between those of the Pacific and Atlantic types. SHL, Southern High Latitude. Leg numbers have been omitted and the two numbers cited are the hole and core numbers.

case following ophiolite emplacement the margin became the site of a major strike-slip system (the proto-Southern Uplands fault).

The depth of burial of the Raven Gill Formation (Leadhills Imbricate Zone) is the key to solving this problem. If the ophiolite had been emplaced over the rocks of the Raven Gill Formation then this formation would have been buried to a depth exceeding 15 km, comprising 10–15 km hot obducted slab plus subsequent sedimentary cover.

Arenig spilites from the Leadhills Imbricate Zone have been metamorphosed to prehnite–pumpellyite facies (300–360°C) at pressures of 1–3 kbar (Hepworth *et al.* 1982; Merriman & Roberts 1996). Caradoc turbidites from the Northern Belt have anchizone (equivalent to the prehnite–pumpellyite facies) illite crystallinity values. Conodonts from the Wrae Limestone (within the Ashgill Shinnel Formation) have a CAI of 5 indicative of heating to 300–400°C (Rejebian *et al.* 1987; Bergström 1980; Armstrong 1997). The apparent

lack of any stratigraphical variation in palaeotemperature between the lower Caradoc and the lower Ashgill is due to the range of temperatures encompassed by the indices. A 100°C range could equate with 3 km depth of burial at normal continental geothermal gradients, the approximate stratigraphical thickness of the preserved Kirkcolm Formation.

The Wrae Limestone is a conglomerate in the Shinnel Formation and its component clasts may have been heated prior to re-deposition. However, the proposed source area for the clasts, to the north of the Southern Upland Fault (the Stinchar Limestone or its approximate lateral equivalents; Owen *et al.* 1996; Armstrong *et al.* 1996; Armstrong 1997) is characterized by low CAI values of 1.5–2 (Bergström 1980). These values are comparable to those of the lowermost Carboniferous and indicate heating to no higher than 80°C and burial to depths of *c.* 2.5 km (Dean & Turner 1995).

The data from the Northern Belt indicate that heating occurred post-early Ashgill. In the absence of significant regional igneous activity of this age it is assumed that the thermal maturity of the sediments was generated by depth of burial. At an average continental geothermal gradient of 30°C km<sup>-1</sup> the recorded temperatures would suggest burial to 10–12 km. This must have been produced by either missing strata (arguments above render this unlikely) or tectonic thickening within the Southern Uplands thrust stack. The combined stratigraphical thickness of the Kirkcolm and Portpatrick formations approaches 5.25 km and thrusting would have to have at least doubled this thickness.

In conclusion, estimates of palaeotemperatures and depth of burial of the Raven Gill Formation indicate the Ballantrae Ophiolite could not have been emplaced over the Leadhills Imbricate Zone. The metamorphic grade of these rocks is best explained in terms of post-early Ashgill tectonic thickening and consequently the Leadhills Imbricate Zone must represent an allochthonous fragment of a marginal basin. If the rocks of the Leadhills Imbricate Zone formed the basement to the later Ordovician cover succession of the Northern Belt of the Southern Uplands (see Leggett 1987) then palaeontological evidence places this terrane adjacent to Pomeroy, Co. Tyrone in the early Caradoc (Owen & Clarkson 1992; Scrutton *et al.* 1998; see also Williams *et al.* 1997).

The apparently anomalously low thermal maturity values of the Girvan area (Bergström 1980) can be explained by the *c.* 2.5 km of preserved Palaeozoic sedimentary cover in this area of the Midland Valley, which must have remained as a positive feature for much of subsequent time. This suggests the Southern Uplands thrust duplex was a highly asymmetrical structure or that the two areas were separated during the initial phase of duplex development. Owen & Clarkson (1992) and Scrutton *et al.* (1998) have argued for <250 km of post-mid-Caradoc sinistral strike-slip between Pomeroy and the Northern Belt of the Southern Uplands.

The Northern Belt exposes a continuous sedimentary record of Caradoc to upper Ashgill greywackes. Sedimentation was terminated in the Northern Belt when the basin inverted in the late Ashgill as a result of the soft-docking of Avalonia (Stone *et al.* 1987; Pickering *et al.* 1988; Armstrong *et al.* 1996). It would therefore seem likely that the emplacement of the Southern Uplands was initiated during the late Ashgill.

## Conclusions

REE indices of depositional regime are reproducible over a variety of ages, ocean basins, degrees of deformation and metamorphism and present a powerful tool for palaeoceanographic and tectonic reconstructions. The chert REE data presented here support the hypothesis that the Balcreuchan Group of the Ballantrae Complex formed in a large marginal ocean basin close to the Midland Valley margin. The Midland Valley terrane provided a source of continental clastic detritus during the early to mid-Arenig.

The lava and chert association of the Leadhills Imbricate Zone in the Southern Uplands represents a fragment of the proximal part a marginal basin subsequently tectonized during later Caledonian faulting. The depth of burial of the Raven Gill Formation (Leadhills Imbricate Zone) precludes the Ballantrae Complex having been thrust over it. A major sinistral strike-slip fault along the southern margin of the Midland Valley terrane is invoked to facilitate the juxtaposition of these two Arenig successions.

We propose a model for the early Ordovician evolution of the Laurentian–Midland Valley margin during which the Ballantrae Ophiolite formed in a marginal basin above a northerly dipping subduction zone. The ophiolite was obducted during the late Arenig (*c.* 470 Ma) following the closure of this basin. Arenig rocks of the Leadhills Imbricate Zone formed part of a marginal basin close to the continental margin and were adjacent to Pomeroy, Co. Tyrone. These rocks formed the basement of the Northern Belt basin which accumulated sediment until the late Ashgill. This basin was inverted and translocated northeastwards along the Midland Valley margin to its present location from the late Ashgill.

J. Pearce is thanked for discussions on REE geochemistry and ophiolite tectonic settings. B. Bluck kindly read and improved an early version of this manuscript. The helpful comments of J. Menuge and an anonymous referee are gratefully acknowledged. C. Ottley and Y. Brown ran the ICP-MS and XRF samples, M. McLeod undertook the XRD analyses and K. Atkinson drew the diagrams; their efforts were much appreciated. This work was undertaken in the context of a British Geological Research Contract held by A.W.O. and H.A.A. (GA/94E/32) which is gratefully acknowledged. This paper is published by permission of the Director, British Geological Survey (NERC).

## References

- AITCHISON, J.C. 1988. A Lower Ordovician (Arenig) radiolarian fauna from the Ballantrae Complex, Scotland. *Scottish Journal of Geology*, **34**, 73–81.
- ARMSTRONG, H.A. 1997. Conodonts from the Shinnel Formation, Tweeddale Member (middle Ordovician), Southern Uplands, Scotland. *Palaeontology*, **40**, 763–799.
- & DEAN, M.T. 1996. Conodonts from Ruddenleys, Lamancha and Crawford, Southern Uplands, Scotland. *British Geological Survey Technical Report*, **WH 96/192 R**.
- , CLARKSON, E.N.K. & OWEN, A.W.A. 1990. A new Lower Ordovician conodont fauna from the Northern Belt of the Southern Uplands of Scotland. *Scottish Journal of Geology*, **26**, 47–52.
- , OWEN, A.W., SCRUTTON, C.T., CLARKSON, E.N.K. & TAYLOR, C.M. 1996. Evolution of the Northern Belt, Southern Uplands: implications for the Southern Uplands controversy. *Journal of the Geological Society, London*, **153**, 197–205.
- BARRETT, T.J., JENKYN, H.C., LEGGETT, J.K. & ROBERTSON, A.H.F. 1982. Comment on "Age and origin of Ballantrae ophiolite and its significance to the Caledonian orogeny and the Ordovician time scale". *Geology*, **10**, 331.
- BERGSTRÖM, S.M. 1980. Conodonts as paleotemperature tools in Ordovician rocks of the Caledonides and adjacent areas in Scandinavia and the British Isles. *Geologiska Föreningens i Stockholm Förhandlingar*, **102**, 377–392.

- BLUCK, B.J. 1978. Geology of a continental margin 1: the Ballantrae complex. In: BOWES, D.R. & LEAKE, B.E. (eds) *Crustal evolution in northwestern Britain and adjacent regions*. Geological Journal, Special Issue, **10**, 151–162.
- 1992a. The Ballantrae Complex. In: LAWSON, J.D. & WEEDON, D.S. (eds) *Geological Excursions around Glasgow and Girvan*. Geological Society of Glasgow, 309–318.
- 1992b. Bennane Head to Downan Point. In: LAWSON, J.D. & WEEDON, D.S. (eds) *Geological Excursions around Glasgow and Girvan*. Geological Society of Glasgow, 347–361.
- , HALLIDAY, A.N., AFTALION, M. & MACINTYRE, R.M. 1980. Age and origin of the Ballantrae ophiolite and its significance to the Caledonian orogeny and Ordovician time scale. *Geology*, **8**, 492–495.
- BORTHWICK, G.W. 1993. Leadhills and Wanlockhead. In: MCADAM, A.D., CLARKSON, E.N.K. & STONE, P. (eds) *Scottish Borders Geology: An Excursion Guide*. Scottish Academic Press, Edinburgh, 192–200.
- BOYNTON, W.V. 1984. Cosmochemistry of the Rare Earth Elements. In: HENDERSON, P. (ed.) *Rare Earth Element Geochemistry*. Developments in Geochemistry, **2**. Elsevier, 63–114.
- CHURCH, W.R. & GAYER, R.A. 1973. The Ballantrae ophiolite. *Geological Magazine*, **110**, 497–510.
- DEAN, M.T. & TURNER, N. 1995. Conodont colour alteration index (CAI) values for the Carboniferous of Scotland. *Transactions of the Royal Society of Edinburgh: Earth Sciences*, **85**, 211–220.
- DEWEY, J.F. & SHACKLETON, R.M. 1984. A model for the evolution of the Grampian tract in the early Caledonides and Appalachians. *Nature*, **312**, 115–121.
- ELDERFIELD, H. & GREAVES, M.J. 1982. The rare earth elements in seawater. *Nature*, **296**, 214–219.
- ETHINGTON, R.L. & AUSTIN, R.L. 1993. A note on the use of hydrofluoric acid for the recovery of conodonts from Ordovician cherts in the Southern Uplands of Scotland and the significance of the conodonts. *Journal of Micropalaeontology*, **12**, 194.
- FLOYD, J.D. 1994. The derivation and definition of the “Southern Upland Fault”: a review of the Midland Valley-Southern Upland terrane boundary. *Scottish Journal of Geology*, **30**, 51–62.
- 1996. Lithostratigraphy of the Ordovician rocks in the Southern Uplands: Crawford Group, Moffat Shale Group, Leadhills Supergroup. *Transactions of the Royal Society of Edinburgh: Earth Sciences*, **86**, 153–165.
- FORTEY, R.A., HARPER, D.A.T., INGHAM, J.K., OWEN, A.W. & RUSHTON, A.W.A. 1995. A revision of the Ordovician Series and Stages in the historical type area. *Geological Magazine*, **132**, 15–30.
- GIRTY, G.H., RIDGE, D.L., KNAK, C., JOHNSON, D. & AL-RYAMI, R. 1996. Provenance and depositional setting of Paleozoic chert and argillite, Sierra Nevada, California. *Journal of Sedimentary Research*, **66**, 107–118.
- HEPWORTH, B.C. 1981. *Geology of the rocks between Leadhills and Abington, Lanarkshire*. PhD thesis. University of St Andrews.
- , OLIVER, G.J.H. & MCMURTRY, M.J. 1982. Sedimentology, volcanism, structure and metamorphism of a Lower Palaeozoic accretionary complex; Bail Hill-Abington area of the Southern Uplands of Scotland. In: LEGGETT, J.K. (ed.) *Trench-Forearc Geology: Sedimentation and Tectonics on Modern and Ancient Active Plate Margins*. Geological Society, London, Special Publications, **10**, 521–533.
- HESSE, R. 1988. Origin of chert: diagenesis of biogenic siliceous sediment. *Geoscience Canada*, **15**, 171–192.
- HOLSER, W.T. 1997. Evaluation of the application of rare-earth elements to paleoceanography. *Palaeogeography, Palaeoclimatology, Palaeoecology*, **132**, 309–323.
- JONES, C.M. 1977. *The Ballantrae complex as compared to the ophiolites of Newfoundland*. PhD thesis, University of Wales.
- JONES, D.L. & MURCHEY, B. 1986. Geologic significance of Palaeozoic and Mesozoic radiolarian chert. *Annual Reviews of Earth and Planetary Sciences*, **75**, 225–237.
- LAMONT, A. & LINDSTRÖM, M. 1957. Arenigian and Llandeilian cherts identified in the Southern Uplands of Scotland by means of conodonts, etc. *Transactions of the Geological Society of Edinburgh*, **17**, 60–70.
- LEGGETT, J.K. 1978. *Studies in the Ordovician rocks of the Southern Uplands, with particular reference to the Northern Belt*. D.Phil. thesis, University of Oxford.
- 1987. The Southern Uplands as an accretionary prism: the importance of analogues in reconstructing palaeogeography. *Journal of the Geological Society, London*, **144**, 737–752.
- & CASEY, D.M. 1982. The Southern Uplands Accretionary Prism: Implications for Controls on Structural Development of Subduction Complexes. In: DRAKE, C.L. & WATKINS, J.S. (eds) *Continental Margin Processes*. American Association of Petroleum Geologists, **24**, 377–393.
- , MCKERROW, W.S. & EALES, M.H. 1979. The Southern Uplands of Scotland: A Lower Palaeozoic accretionary prism. *Journal of the Geological Society, London*, **136**, 755–770.
- LEWIS, A.D. 1975. *The geochemistry and geology of the Girvan Ballantrae ophiolite and related Ordovician volcanics in the Southern Uplands of Scotland*. PhD thesis, University of Wales.
- & BLOXHAM, T.W. 1977. Petrotectonic environments of the Girvan-Ballantrae lavas from rare-earth element distributions. *Scottish Journal of Geology*, **13**, 211–222.
- LÖFGREN, A. 1978. Arenigian and Llanvirnian conodonts from Jämtland, northern Sweden. *Fossils and Strata*, **13**, 1–129.
- MCLENNAN, S.M., TAYLOR, S.R., MCCULLOCH, M.T. & MAYNARD, J.B. 1990. Geochemical and Nd-Sr isotopic composition of deep-sea turbidites: Crustal evolution and plate tectonic associations. *Geochimica et Cosmochimica Acta*, **54**, 2015–2050.
- MERRIMAN, R.J. & ROBERTS, B. 1996. Metamorphism of Lower Palaeozoic rocks. In: STONE, P. (ed.) *Geology in south-west Scotland*. British Geological Survey, 13–15.
- MURRAY, R.W. 1994. Chemical criteria to identify the depositional environment of chert: general principles and applications. *Sedimentary Geology*, **90**, 213–232.
- , BUCHHOLTZ TEN BRINK, M.R., GERLACH, D.C., RUSS, D.P. & JONES, D.L. 1991. Rare earth, major and trace elements in chert from the Franciscan Complex and Monterey Group, California: Assessing REE sources to fine grained marine sediments. *Geochimica et Cosmochimica Acta*, **55**, 1875–1895.
- , —, — & — 1992. Interoceanic variation in the rare earth, major, and trace element depositional chemistry of chert: Perspectives gained from the DSDP and ODP record. *Geochimica et Cosmochimica Acta*, **56**, 1897–1913.
- , —, JONES, D.L., GERLACH, D.C. & RUSS, D.P. 1990. Rare earth elements as indicators of different marine depositional environments in chert and shale. *Geology*, **18**, 268–271.
- OWEN, A.W. & ARMSTRONG, H.A. 1997. Geochemistry and biostratigraphy of Southern Upland Cherts. *British Geological Survey Technical Report WAI 97/48*.
- & CLARKSON, E.N.K. 1992. Trilobites from Kilbucho and Wallace’s Cast and the location of the Northern Belt of the Southern Uplands during the late Ordovician. *Scottish Journal of Geology*, **28**, 3–17.
- , ARMSTRONG, H.A. & FLOYD, J.D. 1999. Rare Earth Element geochemistry of upper Ordovician cherts from the Southern Uplands. *Journal of the Geological Society London*, **156**, 191–204.
- , HARPER, D.A.T. & CLARKSON, E.N.K. 1996. The trilobites and brachiopods of the Wrae Limestone, an Ordovician limestone conglomerate in the Southern Uplands. *Scottish Journal of Geology*, **32**, 133–149.
- PICKERING, K.T., BASSETT, M.G. & SIVETER, D.J. 1988. Late Ordovician–Early Silurian destruction of the Iapetus Ocean: Newfoundland, British Isles and Scandinavia: A discussion. *Transactions of the Royal Society of Edinburgh: Earth Sciences*, **79**, 361–382.
- REJEBIAN, V.A., HARRIS, A.G. & HUEBNER, J.S. 1987. Conodont color and texture alteration: An index to regional metamorphism, contact metamorphism and hydrothermal alteration. *Geological Society of America Bulletin*, **99**, 471–479.
- SCRUTTON, C.T.S., JERAM, A.J. & ARMSTRONG, H.A. 1998. Kilbuchophyllid corals from the Ordovician (Caradoc) of Pomeroy, Co. Tyrone: implications for coral phylogeny and for movement on the Southern Uplands Fault. *Transactions of the Royal Society of Edinburgh: Earth Sciences*, **88** [for 1997], 117–126.
- SEARLE, M.P. & STEVENS, R.K. 1984. Obduction processes in ancient, modern and future ophiolites. In: GASS, I.G., LIPPARD, S.J. & SHELTON, A.W. (eds) *Ophiolites and Oceanic Lithosphere*. Geological Society, London, Special Publications, **13**, 303–321.
- SMELLIE, J.L. 1984. Metamorphism of the Ballantrae Complex, south-west Scotland: a preliminary study. *Report of the British Geological Survey*, **16**, 13–17.
- & STONE, P. 1992. Geochemical control on the evolutionary history of the Ballantrae Complex, SW. Scotland, from comparisons with recent analogues. In: PARSON, L.M., MURTON, B.J. & BROWNING, P. (eds) *Ophiolites and their Modern Oceanic Analogues*. Geological Society Special Publications, **60**, 171–178.
- SMITH, J. 1907. On the occurrence of conodonts in the Arenig-Llandeilo Formations of the Southern Uplands. *Transactions of the Natural History Society of Glasgow*, **7**, 235–252.
- STONE, P. & RUSHTON, A.W.A. 1983. Graptolite faunas from the Ballantrae ophiolite complex and their structural implications. *Scottish Journal of Geology*, **19**, 297–310.

- & SMELLIE, J.L. 1988. *Classical areas of British geology: the Ballantrae area: description of the solid geology of parts of 1:25 000 sheets NX08, 18 and 19*. HMSO, British Geological Survey.
- & — 1990. The Ballantrae Ophiolite, Scotland: an Ordovician island arc-marginal basin assemblage. In: MALPAS, J., MOORES, E.M., PANAYIOTOU, A. & XENOPHONTOS, C. (eds) *Ophiolites: oceanic and crustal analogues*. Geological Survey Department, Nicosia, Cyprus, 535–546.
- , FLOYD, J.D., BARNES, R.P. & LINTERN, B.C. 1987. A sequential back-arc and foreland basin thrust duplex model for the Southern Uplands of Scotland. *Journal of the Geological Society, London*, **144**, 753–764.
- TAYLOR, S.R. & MCLENNAN, S.M. 1985. *The Continental Crust: Its Composition and Evolution*. Blackwell, Oxford.
- THIRLWALL, M.F. & BLUCK, B.J. 1984. Sr-Nd isotope and chemical evidence that the Ballantrae 'ophiolite', SW Scotland, is polygenetic. In: GASS, I.G., LIPPARD, S.J. & SHELTON, A.W. (eds) *Ophiolites and Oceanic Lithosphere*. Geological Society, London, Special Publications, **13**, 215–231.
- WILDE, P., QUINBY-HUNT, M.S. & ERDTMANN, B.-D. 1996. The whole-rock cerium anomaly: a potential indicator of eustatic sea-level changes in shales of the anoxic facies. *Sedimentary Geology*, **101**, 43–53.
- WILKINSON, J.M. & CANN, J.R. 1974. Trace elements and tectonic relationships of basaltic rocks in the Ballantrae igneous complex, Ayrshire. *Geological Magazine*, **111**, 35–41.
- WILLIAMS, D.M., HARKIN, J. & RICE, A.H.N. 1997. Umbers, ocean crust and the Irish Caledonides: terrane transpression and the morphology of the Laurentian margin. *Journal of the Geological Society, London*, **154**, 829–838.

Received 9 April 1998; revised typescript accepted 14 September 1998.  
Scientific editing by Peter Haughton.